

Modeling of Small Scale Solar Power Plant for Electricity and Cooling Production

Mohamed H. Ahmed¹, Amr M. A. Amin²

¹Solar Energy Department, National Research Centre, Giza, Egypt.

²Academy of Scientific Research and Technology ASRT, Cairo, Egypt.

Abstract – Small-scale solar power plants have received a lot of attention recently. In this work, a numerical model was developed to simulate the performance of a solar thermal power plant consists of parabolic trough collector (PTC) with an absorption chiller and an Organic Rankine Cycle (ORC). The numerical model investigates the effect of the operating parameters and meteorological conditions of Cairo on the performance of the plant components. The Therminol-VP1 was used as a storage media in a sensible heat storage tank and also as a heat transfer fluid. The flow rate of the oil through the solar collectors ranges from 0.9 to 1.8 kg/s. The same oil was used also as a heating fluid for the organic Rankine cycle ORC and the absorption chiller with a flow rate range from 0.3 to 0.9 kg/s. Four operating modes for the plant which is an electric generation, heating, cooling, and electric generation with heating mode were investigated. The model examines the impact of these operating modes on the plant performance. The maximum thermal power produced by the PTC in winter and summer was about 74 and 127 KW respectively. The numerical model proved also that the designed plant can collect thermal energy ranges from 632 to 1185 kWh from Jan. to Jun., respectively. The daily electric energy produced by the plant range from 45.6 – 85.5 kWh for the same period.

Key Words: Solar thermal plant; Parabolic trough collector; Organic Rankine Cycle; Absorption chiller, Modelling

1. INTRODUCTION

Due to the energy crisis and increasing the demand for electricity in the world the scientists turn to search for other sources of energy that can generate electricity. The solar energy comes as the best renewable and sustainable source of energy. The Concentrated Solar Power (CSP) system is considered as one of the most promise methods to utilize solar energy. CSP is a mechanism that uses a mirror to concentrate the solar irradiance on a small area [1]. Several CSP plants have been installed in several countries such as Egypt, Spain, Italy, Morocco, Algeria, and USA [2]. Using solar irradiance as a thermal energy source for electricity generation has several advantages such as being a clean and renewable source of energy. Most thermal systems used to generate electricity are based on a steam Rankine cycle that needs high temperatures and pressure. The temperature and pressure required for the steam Rankine cycle are higher than 500 °C and 80 bar, respectively. The organic Rankine cycle (ORC) came as a good and easy solution to generate

electricity at low temperature and pressure levels. ORCs offer a renewable electric power production opportunity using low-temperature heat sources [3]. The ORC can be powered from low-grade heat sources such as industrial waste heat [4], geothermal [5], ocean thermal [6], biomass [7] and solar energy [8–10]. The working fluid type is considered as the main difference between conventional Rankine cycles (RCs) and ORCs [11]. The scientists took great interest in the development of the ORC by recovering the waste energy, as well as using the newly developed refrigerant R-245fa [12, 13]. Also, many ORCs operate at lower pressures, which reduce the capital cost of components. Solar energy can serve many applications in our public life such as electricity generation, air conditioning, desalination and water heating ...etc. Installing a Solar thermal plant to serve more than one application is a good way to raise the efficiency of the plant and increase its economic. So that using absorption chiller for achieving cooling for an air conditioning system is an appropriate method for exploitation the solar heat energy, which is compatible with the demand for cooling. Meanwhile, an oil-water heat exchanger is used to capture the heat energy from the Storage media in the tank to achieve a space heating in winter. There are different types of the CSP that used in the solar power plant and have achieved a success in Europe, the Middle East and North Africa [14, 15].

In this research article, the potential of the PTC to power different machines such as ORC, absorption chiller and a heat exchanger have been investigated. The study of the cogeneration, i.e. the simultaneous production of electrical and thermal energy (cooling and heating) is the aim of this research. The study aims to investigate the effect of the operating parameters and metrological condition the thermal performance of the plant in terms of the outlet temperature, energy gained, electricity production, and plant efficiency. Also, the aim of this research is to develop a numerical model for the small-scale multi-application solar power plant. The other objective is to evaluate theoretically the performance of this cogeneration plant under the climate of Egypt over an annual period and at different operations mode. Four operation modes such as electricity generation, cooling, heating, and electricity generation plus heating were used through the theoretical investigation

2. SYSTEM DESCRIPTION

The main parts of the small-scale solar power plant are the solar collector field, storage tank, the organic Rankine cycle, absorption chiller, and heat exchanger. Fig. 1 illustrates a schematic diagram of the solar plant including its main components. The solar field consists of parabolic trough concentrators supported by a single-axis tracking system. The concentrators are arranged in parallel rows and its axis of rotation aligned on a north-south direction. Each concentrator contains reflective mirrors in the form of a linear parabola that focuses the direct solar beam radiation on a linear evacuated receiver tube located at the focus line of the parabola. The concentrator tracks the sun from east to west during the day with the help of a tracking system to ensure a continuous focus of solar radiation on the receiving tube. The temperature of the heat transfer fluid (HTF) increases as it passes through the receiver tube and then the HTF returns to a storage tank using a circulating pump. The HTF, the storage media inside the tank and the fluid flowing to the applications is the thermal oil. The cogeneration plant can be operated in four different operating modes which are an electric generation, cooling, heating and electric generation, and heating mode. In the electric generation mode, the hot oil flows through the ORC's evaporator. The oil vaporizes the working fluid into a superheated vapor. For the cooling mode, the hot oil flow to the absorption chiller for increasing the concentration of the absorption solution in the generator then return back to the storage tank. In the heating mode, the heat exchanger transfers the heat from the oil to water which can be used for space heating. In the electric generation with the heating mode, the hot oil comes out from the evaporator in the ORC flow to the heat exchanger.

increases as it passes through the receiver tube and then the HTF returns to a storage tank using a circulating pump. The HTF, the storage media inside the tank and the fluid flowing to the applications is the thermal oil. The cogeneration plant can be operated in four different operating modes which are an electric generation, cooling, heating and electric generation, and heating mode. In the electric generation mode, the hot oil flows through the ORC's evaporator. The oil vaporizes the working fluid into a superheated vapor. For the cooling mode, the hot oil flow to the absorption chiller for increasing the concentration of the absorption solution in the generator then return back to the storage tank. In the heating mode, the heat exchanger transfers the heat from the oil to water which can be used for space heating. In the electric generation with the heating mode, the hot oil comes out from the evaporator in the ORC flow to the heat exchanger.

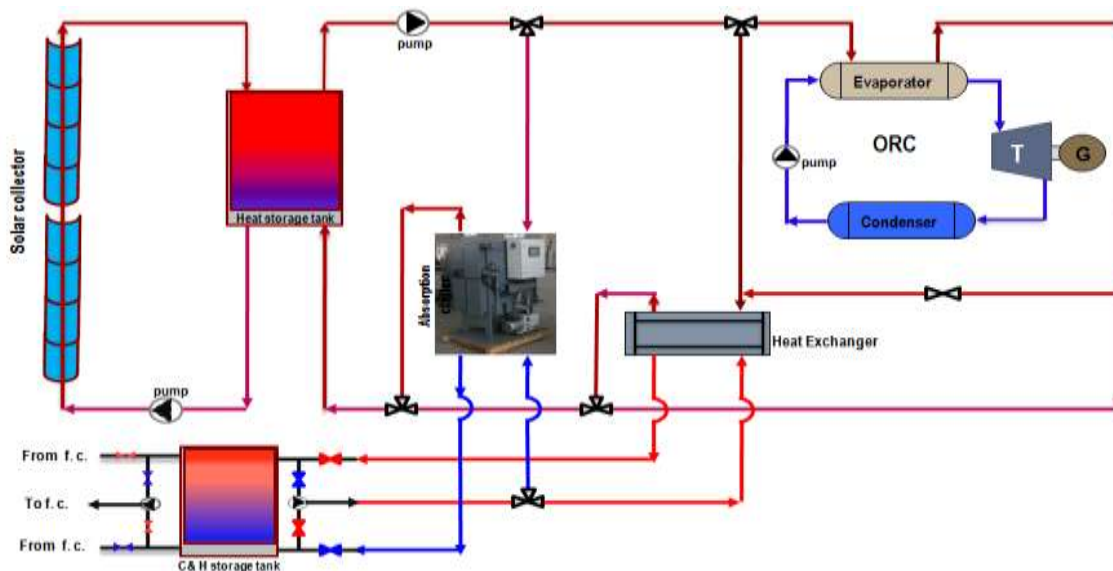


Fig -1: A Schematic diagram for a cogeneration solar plant

The organic Rankine cycle contains four main parts: evaporator, condenser, a pump, and a turbine. The organic Rankine cycle principle depends on the turbine generator that acts as a traditional steam turbine to convert thermal energy into mechanical energy and then to electric energy through an electric generator. The ORC is fed with hot oil to heat and vaporize an organic working fluid to a superheated state in the evaporator. The exhaust superheated vapor from the evaporator rotates the turbine, which is directly coupled to the electric generator, leads to electricity generation. The outlet vapor from the turbine is then condensed through the condenser using a cooling water circuit. The organic working fluid is then pumped into the evaporator, consequently completing the process of the closed-cycle. The superheat process is indispensable in order to maintain that in the fluid inside the turbine is only vapor, thus preserving the turbine blades from condensation and erosion. However, the overheating process should not increase much to avoid wasted energy and maximize circuit performance. The

working fluids that used in the ORC are organic fluids. The most important specification required for organic liquid is to have low latent heat, low density, and low evaporation temperature. These specifications are important to increase the inlet mass flow rate to the turbine and minimize the heat consumed in the evaporation process. The organic fluids R-134a, R-123, and R-245fa are the most common working fluids that can be used. The performance of the cycle is affected by the properties of the selected working fluid. The appropriate selection of the working fluid has a significant effect on improving the ORC.

3. NUMERICAL MODELING

The numerical model of the plant component was build using the engineering equation solver EES. Each component of the plant was simulated separately and then connected with other components.

3.1 Modeling of PTC collector

A numerical model was built to model the radiation energy incident on the parabolic reflected mirror and the reflected radiation absorbed by the receiver tube. It also simulated the heat energy generated due to the radiation absorbed by the steel tube as shown in Fig. 2. The energy transferred by conduction, radiation, and convection from the absorber tube to the glass cover and the heat transfer fluid HTF was also simulated using the energy balance equations for each of the steel tube, glass cover and the HTF [16]. The model simulates the convection and radiation heat losses from the absorber tube to the glass envelope. It predicts also the heat transfer by conduction from the inner to the outer surface of the glass cover. The convection and radiation heat losses from the glass envelope outer surface to the ambient by were also considered in the modeling.

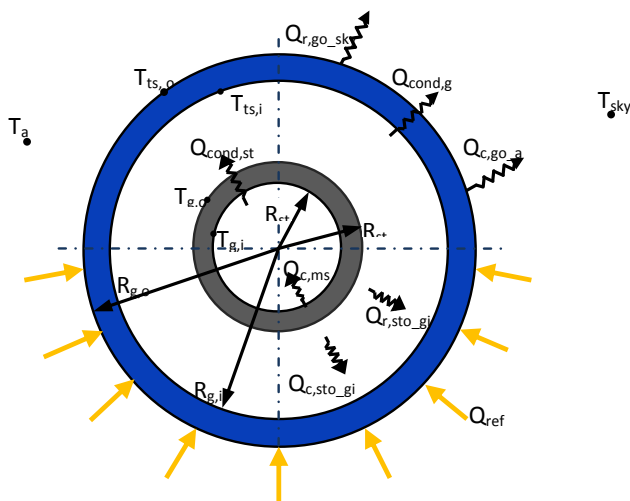


Fig -2: A Schematic of the numerical model for the receiver tube

3.2 Modeling of the storage tank

The storage tank was modeled as a transient one-dimensional stratified tank. The tank height was divided into segments of thickness Δx as shown in Fig. 3. The interior heat convection and conduction between the tank segments was considered. The thermal losses from the tank surface as well as mixing at the tank inlet and outlet boundaries were also considered in the model during the charging and discharging mode [17]. The tank model takes into consideration all the forms of energy coming in and out of the segment by arranging the coefficients of T_{i-1} , T_i and T_{i+1} , the segment energy balance takes the following equation:

$$a_i T_{i-1} + b_i T_i + c_i T_{i+1} + d_i = 0 \quad (1)$$

Where T_{i-1} , T_i and T_{i+1} are the segments temperature. The coefficients a , b , c , and d are computed from the heat and mass transfer equations.

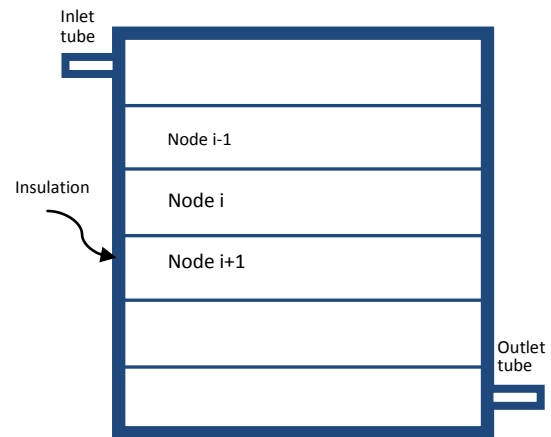


Fig -3: A schematic diagram of the storage tank with segments

3.3 Modeling of the ORC

Modeling of the ORC depends on modeling of all components forming the cycle as shown in Fig. 4. The evaporator and the condenser were treated as a two-phase heat exchanger. The turbine and plume were simulated with the isentropic process the components parameters were selected for the available component in the market. In the evaporator, one-dimensional heat transfer was assumed between the two heat transfer fluids. The thermal oil represents the heating source fluid which flows in the evaporator as one phase flow, while the organic fluid represents the cold fluid and passes through the evaporator in the different three phases (liquid, two-phase and vapor phase). So that, the evaporator length was divided into three main zones which are puro liquid zone, mixed zone and the vapor zone each zone was treated as a separated heat exchanger. The heat losses from the heat exchangers are neglected, the amount of the heat added to the working fluid in time is equal to the heat extracted from the heating fluid. For design and performance calculations, the Effectiveness-Number of Heat Transfer Unit (NTU) method was used without iteration. For each zone the inlet temperature for the hot and the cold fluid stream are $T_{h,i}$ and $T_{c,i}$, respectively and the outlet temperature for hot and cold streams are $T_{h,o}$ and $T_{c,o}$, respectively. The outlet fluids temperatures were calculated from the following equations:

$$\dot{Q} = \varepsilon \dot{Q}_{max} \quad (2)$$

$$\dot{Q} = \dot{m}_h C_{p_h} (T_{h,i} - T_{h,o}) = \dot{m}_c C_{p_c} (T_{c,o} - T_{c,i}) \quad (3)$$

Where:

- \dot{Q} The actual heat transfer rate (kW)
- \dot{Q}_{max} The maximum possible heat transfer rate (kW).
- ε Effectiveness
- \dot{m}_h The mass flow rates of the hot fluid (kg/s)
- \dot{m}_c The mass flow rates of the cold fluid (kg/s)
- C_{p_h} The specific heat of the hot fluid (kJ/kg k)

C_{pc} The specific heat of the cold fluid (kJ/kg k)

The effectiveness ϵ for the single and the two-phase zones are calculated using the following equations:

$$\epsilon = \frac{1 - \exp(-NTU(1 - C_r))}{1 - C_r(-NTU(1 - C_r))} \quad (4)$$

$$\epsilon_{tp} = 1 - \exp(-NTU) \quad (5)$$

Where C_r is the heat capacity ratio $C_r = \dot{C}_{min} / \dot{C}_{max}$

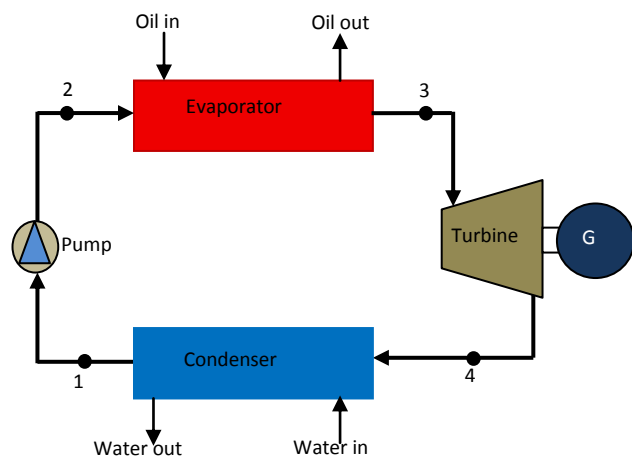


Fig -4: A schematic diagram of the ORC

The working fluid heated in the evaporator to superheated vapor at constant pressure (evaporating pressure). The heat transfer rate from the evaporator \dot{Q}_e into the working fluid is given by:

$$\dot{Q}_e = \dot{m}_f (h_3 - h_2) \quad (6)$$

The superheated vapor passes through the turbine to generate the mechanical power. The power output from the \dot{W}_t turbine is given by:

$$\dot{W}_t = \dot{m}_f (h_3 - h_4) \quad (7)$$

The vapor outside of the turbine flows into the condenser where it is condensed by cooling water. The rate of heat removed by the condenser \dot{Q}_c can be expressed as:

$$\dot{Q}_c = \dot{m}_f (h_4 - h_1) \quad (8)$$

The pump power \dot{W}_p can be expressed as:

$$\dot{W}_p = \dot{m}_f (h_2 - h_1) \quad (9)$$

Where \dot{m}_f is the mass flow rate of the working fluid (kg/s)
 h is the enthalpy (kJ/kg)

3.3 Modeling of the absorption chiller

The absorption chiller used in the modeling is a single effect type that uses the lithium bromide - water LiBr-water as a working solution. This type of absorption chiller operates at temperature ranges from 90 to 120 °C. The mathematical modeling was performed at zero-dimensional energy and mass balancing. The equations used in the modeling for the evaporator, absorber, generator, and condenser are referred to that presented by Worble et al [18].

For simplification purpose, the steady state condition is assumed for all components. The characteristic of the PTC, ORC and the absorption chiller with the operating conditions are presented in table 1.

Table -1: Sample of the input data for the model.

Parameter	Quantity	Unit
PTC collector		
Parabola width	2.4	m
Parabola length	9.9	m
Module area	23.76	m ²
No. of PTC module	8	module
Total mirror area	190.0	m ²
Mirror reflectivity	0.95	-
Glass transmissivity	0.94	-
Receiver tube absorptivity	0.88	-
ORC		
Capacity	6.5	KW
Turbine isentropic efficiency	85	%
Pump isentropic efficiency	75	%
Working fluid	R123	-
Inlet hot oil temperature	150	°C
outlet hot oil temperature	103	°C
Hot oil flow rate	0.6	kg/s
Inlet cooling water temperature	25	°C
outlet cooling water temperature	30	°C
Evaporating pressure	450	Kpa
Condensing pressure	120	Kpa
Absorption chiller		
Mode	Single effect	-
Working fluids	Li Br - Water	-
Inlet hot oil temperature	120	°C
Outlet hot oil temperature	85	°C
Capacity	35	KW
COP	0.55	-

4. RESULTS AND DISCUSSIONS

The performance of the parabolic trough collector during the 1st half year will be presented in the following section. Fig. 5 shows the rate of heat energy gained from the PTC that was calculated for the different months of the year at an inlet temperature of 100 °C, respectively. From the figures we can observe that an output energy rate of about 74 kW can be obtained at Jan. with a big fluctuation between 8 a.m. and 5 p.m. the fluctuation is due to the high radiation incident angle at solar noon during the winter months where these phenomena appear also for Feb. and Mar. with a smaller fluctuation. We can also observe an output energy rate of about 127 kW with nearly no fluctuation in Jun. at solar noon due to the small radiation incident angle. From the figure, we can see an increase in the rate of energy gained from Jan. to Apr., while it seems to be the same for the summer months from Apr. to Jun.

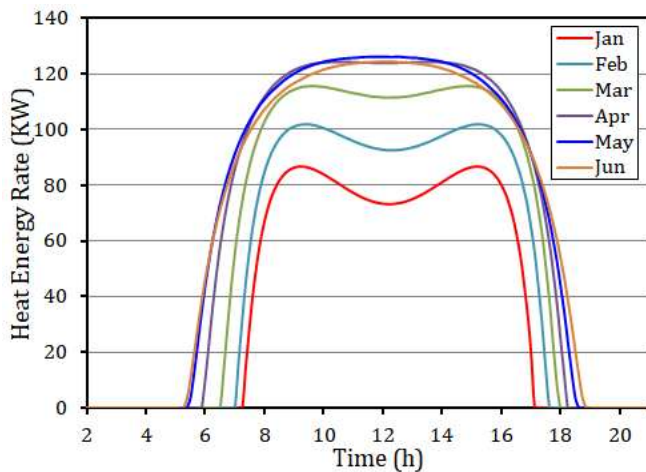


Fig -5: The output thermal energy of the PTC, $T_{in} = 100\text{ }^{\circ}\text{C}$

At the inlet temperature of about 100 C, The effect of the mass flow rate on the outlet temperature is shown in Fig. 6 for different months all over the year. For a mass flow rate of about 1.75 kg/s, an outlet temperature of about 121 to 134 °C can be obtained at solar noon from Jan to Jul, respectively. While for a mass flow rate of 1 kg/s, the outlet temperatures of about 137 to 159 °C can be obtained at solar noon from Jan. to Jul., respectively. From the figure, we can observe an increase in the outlet temperature due to decrease the mass flow rate this observation is evidenced at the summer months.

The accumulation energy gained and the direct normal irradiance through one day are presented in Fig. 7. The daily energy gained from the PTC change from 632 to 1185 kWh for corresponding incident normal radiation range from 1020 to 1675 kWh from Jan to Jun, respectively. The electricity produced range from 45.6 to 85.5 kWh for the same period.

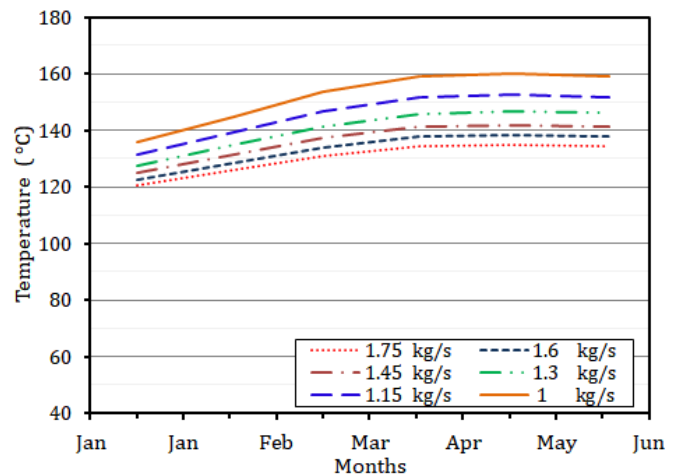


Fig -6: The PTC outlet temperature for different oil mass flow rate

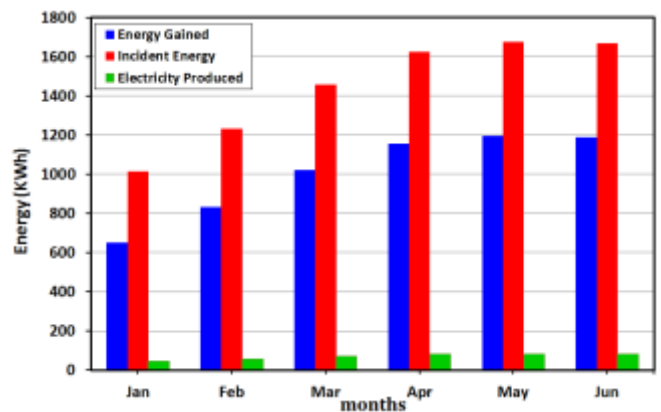


Fig -7: The daily energy gained and the energy incident on

The energy profiles for the storage tank are illustrated in Fig. 8 where the quantity of the heat energy rate stored, withdraw and stored are presented during the cooling operation mode as an example for May. From the figure, it can be observed that the excess energy stored in the storage tank during the period from 5.3 a.m. up to 4.5 p.m. then the cooling machine start to withdraw the heat energy from the tank to compensate the reduction in the heat energy from the PTC up to 6.5 P.m. then the cooling machine depend completely on the power withdrawn from the tank up to 10 p.m.

The overall efficiency of the solar poly-generation plant depends on the operating mode. Fig. 9 presents the plant overall efficiency at the different operating modes. From the figure, we can observe that the heating mode show the highest overall plant efficiency which is 53 %, while the electricity generation mode gives the lowest overall plant efficiency which is 5.5 % due to the high quantity of energy rejected in the condenser of the ORC. The cooling operating mode gives overall plant efficiency of about 38%.

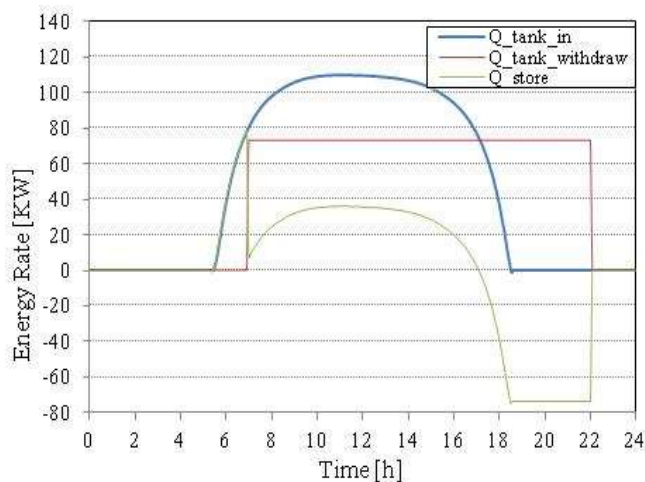


Fig-8: The tank energy feed, withdraw and stored during the cooling mode

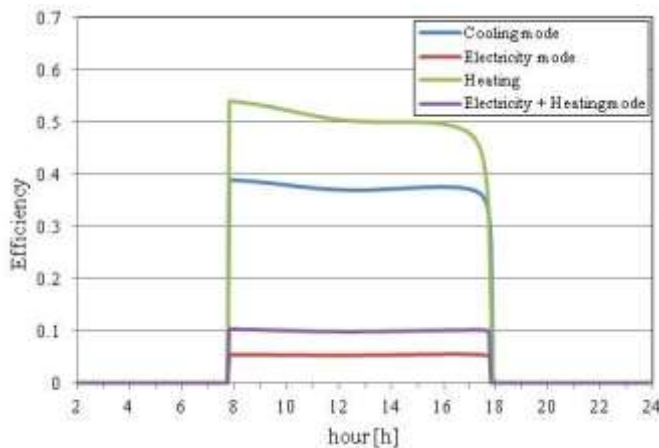


Fig-9: The plant efficiency at the four operating modes through a day in May

4. CONCLUSIONS

The performance of the poly-generation solar power plant using four modes of operation electricity generation, cooling, heating and electric generation plus heating is presented. The thermodynamic modeling of the plant is performed to study the performance of the solar thermal system including the parabolic trough collector and the storage tank. The model studies also the effect of the operating mode on the operation period for the plant. The results of this study are summarized as follow:

- 1) The maximum rate of heat energy gained from the PTC range from 74 to 127 kW for Jan. to Jun., respectively. The fluctuation is due to the incident angle fluctuation through the day represented about 12.5 % during the solar noon period at Jan, while it represents about 1.5 % at Jun.
- 2) The heating operating mode represents the highest plant efficiency where the plant efficiency reaches 53 %, while in the cooling operating mode represent 38.5%, while the

electricity generating operating mode represents the lowest plant efficiency where the plant efficiency is 5.5 %.

- 3) The plant operation period in the case of the space heating mode reaches to 18 h/day, while in the electricity generation mode the plant operates for about 11 h/day.

ACKNOWLEDGEMENT

The authors acknowledge the support of the Academy of Scientific Research and Technology (ASRT). Also, they gratefully acknowledge the support of the European Neighborhood and Partnership Instrument (ENPI) through the STS-med project.

REFERENCES

- [1] I. L. García, J. L. A. lvarez and D. Blanco, "Performance Model for Parabolic Trough Solar Thermal Power Plants with Thermal Storage: Comparison to Operating Plant Data," *Solar Energy*, vol. 85, Oct. 2011., pp. 2443–2460, doi:10.1016/j.solener.2011.07.002
- [2] A. G. Finat and R. Liberali, "Concentrating Solar Power: from Research to Implementation," Luxembourg: European Communities; 2007.
- [3] B. F. Tchanche, G. Lambrinos, A. Frangoudakis and G. Papadakis, "Low-grade heat conversion into power using organic Rankine cycles – a review of various applications," *Renewable and Sustainable Energy Reviews*, vol. 15, No. 8, Oct. 2011, pp. 3963–79, doi:10.1016/j.rser.2011.07.024
- [4] J. P. Roy, M. K. Mishra and A. Misra, "Parametric optimization and performance analysis of a waste heat recovery system using Organic Rankine Cycle," *Energy*, vol. 35, No. 12, Dec. 2010, pp. 5049–5062, doi:10.1016/j.energy.2010.08.013
- [5] D. Tempesti, G. Manfrida and D. Fiaschi "Thermodynamic analysis of two micro CHP systems operating with geothermal and solar energy," *Applied Energy*, vol. 97, Dec. 2012, pp. 609–617, doi:10.1016/j.apenergy.2012.02.012
- [6] S. K. Wang and T. C. Hung, "Renewable energy from the sea – organic Rankine Cycle using ocean thermal energy conversion," *Proceedings of the international conference on energy and sustainable development: issues and strategies (ESD)*, June 2010, pp. 1–8.
- [7] H. Liu, Y. Shao and J. Li, "A biomass-fired micro-scale CHP system with organic Rankine cycle (ORC) – thermodynamic modeling studies," *Biomass and Bioenergy*, vol. 35, No. 9, Oct. 2011, pp. 3985–3994, doi:10.1016/j.biombioe.2011.06.025
- [8] A. M. Delgado-Torres and L. Garcia-Rodriguez, "Analysis and optimization of the low temperature solar organic Rankine cycle (ORC)," *Energy Conversation*

Management, vol. 51, No. 12, Dec. 2010, pp. 2846–2856,
doi:10.1016/j.enconman.2010.06.022

- [9] M. Marion, I. Voicu and A.L. Tiffonnet, "Study and optimization of a solar subcritical organic Rankine cycle," *Renewable Energy*, vol. 48, Dec. 2012, pp. 100–109, doi:10.1016/j.renene.2012.04.047
- [10] R. Rayegan and Y. X. Tao "A procedure to select working fluids for Solar Organic Rankine Cycles (ORCs)," *Renewable Energy*, vol. 36, No. 2, Feb. 2011, pp. 659–670, doi:10.1016/j.renene.2010.07.010
- [11] B. F. Tchanche, G. Papadakis, G. Lambrinos and A. Frangoudakis, "Fluid selection for a low-temperature solar organic Rankine cycle," *Applied Thermal Engineering*, vol. 29, No. 2, Aug. 2009, pp. 2468–2476, doi:10.1016/j.renene.2010.07.010
- [12] G. J. Zyhowski, M. W. Spatz and S. Yana Motta, "An Overview of the Properties and Applications of HFC-245fa," the 9th International Refrigeration and Air Conditioning Conference, at Purdue, West Lafayette, Indiana, July 16-19, 2002.
- [13] J.J. Brasz and B. P. Biederman, "Low Temperature Waste Heat Power Recovery Using Refrigeration Equipment," 21st IIR International Conference of Refrigeration, Washington DC, August 17-22, 2003.
- [14] R. Pitz-Paal et al., "Concentrating Solar Power in Europe, the Middle East and North Africa: Achieving its potential," *Journal of Solar Energy Engineering*, vol. 134, Apr. 2012, pp 24501-1-6, doi:10.1115/1.4006390
- [15] A. Tsikalakis et al., "Review of best practices of solar electricity resources applications in selected Middle East and North Africa (MENA) countries," *Renewable and Sustainable Energy Reviews*, vol. 15, 2011, pp. 2838–2849, doi:10.1016/j.rser.2011.03.005
- [16] M. H. Ahmed, "Two Dimension Numerical Modeling of Receiver Tube Performance for Concentrated Solar Power Plant," *Energy Procedia*, vol. 57, 2014, pp. 551-560, doi:10.1016/j.egypro.2014.10.209
- [17] M. H. Ahmed, "Unsteady Numerical Simulation for Studying The Thermocline Phenomenon Inside a Storage Tank for Molten Salt," *Journal of Applied Science Research*, vol. 8, No. 8, Jan. 2012, pp. 4635- 4644,
- [18] G. A. Florides, S. A. Kalogirou, S.A. Tassou and L. C. Wrobel, "Design and construction of a LiBr-water absorption machine," *Energy Conversion and Management*, vol. 44, Sept. 2003, pp. 2483–2508, doi:10.1016/S0196-8904(03)00006-2